ELSEVIER

Materials Science and Engineering A 449–451 (2007) 198–202

MATERIALS SCIENCE & ENGINEERING A

www.elsevier.com/locate/msea

A study of glass-formation, formation of the supercooled liquid and devitrification behavior of Ni-based bulk glass-forming alloys

Dmitri V. Louzguine-Luzgin *, Takeyuki Shimada, Akihisa Inoue

Institute for Materials Research, Tohoku University, Katahira 2-1-1, Aoba-Ku, Sendai 980-8577, Japan

Received 24 August 2005; received in revised form 22 November 2005; accepted 15 February 2006

Abstract

Glass-formation and devitrification of the glassy phase in the Ni–Nb–Zr–Ti and Ni–Nb–Zr–Ti–NM (NM, noble metals) system alloys exhibiting the supercooled liquid on heating were investigated. The crystallized structure and kinetics of devitrification of Ni–Nb–Zr–Ti–Pd glassy alloy are studied in detail. The formation of the glassy single phase has been proven using high-resolution transmission electron microscopy (TEM). The addition of Zr and Pd increases the supercooled liquid region of the $Ni_{60}Nb_{25}Ti_{15}$ (numbers indicate at.%) alloy from 44 K to about 50 K. The cP2 TiNi phase was found to form during the first exothermic phase transformation in all studied alloys. The addition of Zr to Ni–Nb–Ti alloy prevents formation of oP8 Ni_3Nb phase observed in the $Ni_{60}Nb_{25}Ti_{15}$ alloy and initiates formation of the primary $Ni_{10}Zr_7$ phase while the additions of both NM and Zr effectively refine cP2 TiNi particles size. Definite fractions of rhombohedral R and hR14 Ni_4Ti_3 phases were also observed in NM-bearing alloys. Significantly lower growth rates of the devitrification products in the NM-bearing alloys compared to the Ni–Nb–Ti one may be the reason for the improvement of glass-forming ability (GFA).

Keywords: Glassy alloy; Supercooled liquid; Devitrification; Nanocrystalline material

1. Introduction

Bulk glassy alloys with a size exceeding 1 mm (maximum 100 mm) in three dimensional space were obtained by stabilization of the supercooled liquid against crystallization in the various, mostly multi-component, metallic alloys [1–3]. These alloys are promising materials for structural applications as they exhibit high mechanical strength, high hardness, good fracture toughness, good corrosion resistance and so on [2]. In some alloys partial devitrification of a glassy phase forming nanocrystalline or nanoquasicrystalline precipitates is known to cause its ductilization at definite volume fraction of the precipitates [2].

Recently, bulk glass-formation was achieved in various Ni-base alloy systems: Ni–Zr–Ti–(Si, Sn) [4,5], Ni–Nb–Ti–Zr [6], Ni–Nb–Ti [7], Ni–Nb–Ti–Hf [8,9], Ni–Nb–Sn [10] and so on. They belong to an LTM–ETM or LTM–ETM–M group of alloys (where LTM is(are) late transition metal(s), ETM is(are) early transition metal(s) and M metalloid or Sn). $Ni_{60}Nb_{25}Ti_{15}$ (numbers indicate at.%) bulk glassy alloy showed high ultimate compressive strength of 3085 MPa and plastic deformation of about 2% [7]. Multicomponent Ni–Nb–Ti–Zr–Co–Cu bulk glassy alloy with a critical diameter of 3 mm exhibited high tensile fracture strength of 2700 MPa [11]. Surprisingly $Ni_{59}Zr_{16}Ti_{13}Si_3Sn_2Nb_7$ bulk glassy alloy, produced recently, showed a significant plastic deformation of 6.5% to failure [12]. It allows to suggest that this alloy may contain nanoparticles which are not detectable by an X-ray diffraction (XRD) technique.

It has been also shown that an addition of Ni to Cu-based LTM–ETM glass-forming alloys significantly changes their devitrification behavior [13]. Also contrary to $Cu_{55}Zr_{30}Ti_{10}Pd_5$ alloy [14,15] no icosahedral phase has been observed in $Ni_{55}Zr_{30}Ti_{10}Pd_5$ one [16].

Devitrification (crystallization) behavior of $Ni_{60}Nb_{25}Ti_{15}$ glassy alloy has been studied recently [17]. It has been also found that the addition of noble metals (NM) improves the glass-forming ability (GFA) of the alloy [17]. Kinetic reasons for improvement of GFA may be connected with the growth rate of the crystalline phases, stability of the supercooled liquid, etc. At the same time, devitrification process of multicomponent Ni–Nb–Ti–Zr–NM alloys is poorly studied.

* Corresponding author. Tel.: +81 22 215 2220; fax: +81 22 215 2111.
E-mail address: dml@imr.tohoku.ac.jp (D.V. Louzguine-Luzgin).

0921-5093/$ – see front matter © 2006 Elsevier B.V. All rights reserved.
doi:10.1016/j.msea.2006.02.265

In the present work we study the effect of addition of a 4-d ETM Zr (substituting Nb) and 4-d late transition noble metals, namely Ag and Pd (substituting Ni) on devitrification of the $Ni_{60}Nb_{25}Ti_{15}$ glassy alloy.

2. Experimental procedure

The ingots of nominal compositions $Ni_{60}Nb_{25}Ti_{15}$, $Ni_{60}Nb_{20}Ti_{15}Zr_5$, $Ni_{55}Pd_5Nb_{20}Ti_{15}Zr_5$ and $Ni_{55}Ag_5Nb_{20}Ti_{15}Zr_5$ alloys (at.%) were prepared by arc-melting mixtures of Ni 99.9, Nb 99.9, Zr 99.7, Ti 99.7, Pd 99.9 and Ag 99.9 mass% purities in an argon atmosphere. From these ingots, ribbon samples of about 20 μm in thickness and 1 mm in width were prepared by rapid solidification of the melt on a single copper roller at a roller surface velocity of 42 m/s. The structure of the samples was examined by X-ray diffractometry with monochromatic Cu Kα radiation. The phase transformations were studied by differential scanning calorimetry (DSC) at a heating rate of 0.67 K/s and differential isothermal calorimetry. Transmission electron microscopy (TEM) investigation was carried out using a JEM 2010 (JEOL) microscope operating at 200 kV equipped with an energy dispersive X-ray (EDX) spectrometer of 0.1 keV resolution. The samples for TEM were prepared by the ion-polishing technique.

3. Results

TEM images in Fig. 1 as well as the XRD patterns indicate that the as-solidified alloys have an amorphous structure.

The DSC traces of the ribbon samples demonstrated in Fig. 2(a) show variation of C_p at the onset temperature of the glass transition (T_g) marked with an arrow and the exothermic peaks (A, B and C) due to subsequent crystallization of the supercooled liquid. The addition of Zr and Pd increases the supercooled liquid region of Ni–Nb–Ti alloy from about 45 K to about 50 K.

Compared to the ternary $Ni_{60}Nb_{25}Ti_{15}$ glassy alloy which exhibits competing growth of oP8 Ni_3Nb and cP2 TiNi phases upon crystallization [17] the addition of Zr and NM eliminates Ni_3Nb phase (Fig. 3). Even a small addition of Zr stabilizes oC68 $Ni_{10}(Zr, Ti)_7$ phase which has been observed to form in Ni–Zr–Ti [13], Ni–Zr–Ti–NM [16] and Cu–Zr–Ti–Ni (in the form of $(Cu, Ni)_{10}(Zr, Ti)_7$) [13] alloys. This phase follows precipitation of cP2 TiNi phase in $Ni_{60}Nb_{20}Ti_{15}Zr_5$ alloy (Fig. 3). The lattice parameters of the $Ni_{10}(Zr, Ti, Nb)_7$ solid solution phase in $Ni_{60}Nb_{20}Ti_{15}Zr_5$ alloy obtained by the least squares fitting are: $a = 0.887$ nm, $b = 0.885$ nm, $c = 1.190$ nm, respectively. They are significantly lower than those of the binary $Ni_{10}Zr_7$ phase due to dissolution of Nb and Ti substituting Zr.

The lattice parameter of cP2 TiNi phase in each studied alloy is somewhat smaller than $a = 0.2972$ nm [18] of the binary cP2 TiNi phase without the solute elements. It is the smallest (0.293 nm) in the $Ni_{60}Nb_{25}Ti_{15}$ alloy illustrating that Nb forms a solid solution substituting Ti. It is also confirmed by an energy dispersive X-ray analysis. However, the cP2 binary TiNi symbol will be farther used describing such a solution for simplicity. cP2 TiNi phase in $Ni_{60}Nb_{20}Ti_{15}Zr_5$, $Ni_{55}Ag_5Nb_{20}Ti_{15}Zr_5$ and $Ni_{55}Pd_5Nb_{20}Ti_{15}Zr_5$ alloys has the lattice parameter of 0.294, 0.295 and 0.296 nm, respectively, as determined using (1 1 0) peak in Fig. 3. This also illustrates the effect of the alloying elements: Zr substitutes Ti and Nb while Ag or Pd substitute Ni increasing lattice parameter of cP2 TiNi as the dissolving atoms are larger in size than the dissolvent ones.

One can see that the diffraction peaks of cP2 TiNi phase in Fig. 3 are broadened. It allows to estimate the coherent scattering area size (crystallite size) using a procedure described in Ref. [19] and successfully used in various works, for example in Ref. [16]. The resulted coherent scattering area sizes

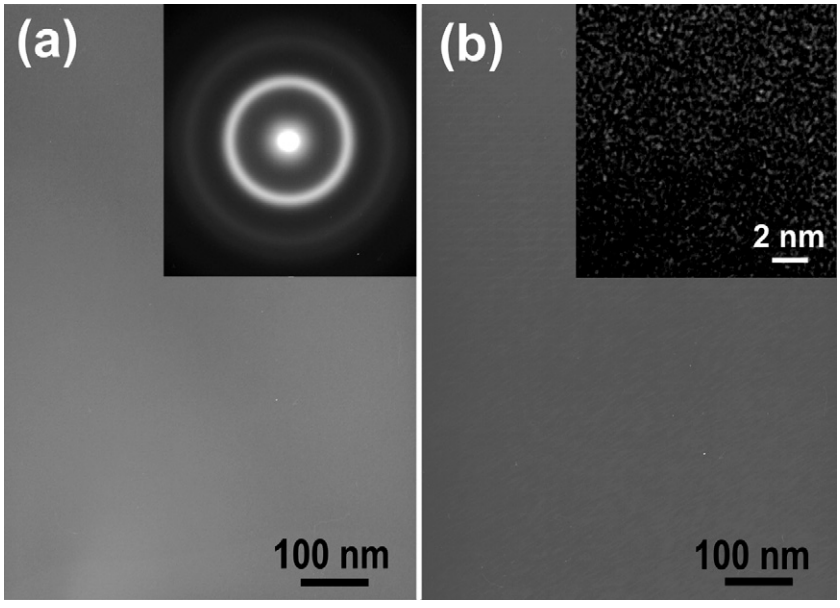

Fig. 1. Structure of $Ni_{55}Pd_5Nb_{20}Ti_{15}Zr_5$ glassy alloy in as-solidified state, TEM. (a) Bright-field image, *inset*: selected-area electron diffraction pattern. (b) dark-field image, *inset*: high-resolution TEM image.

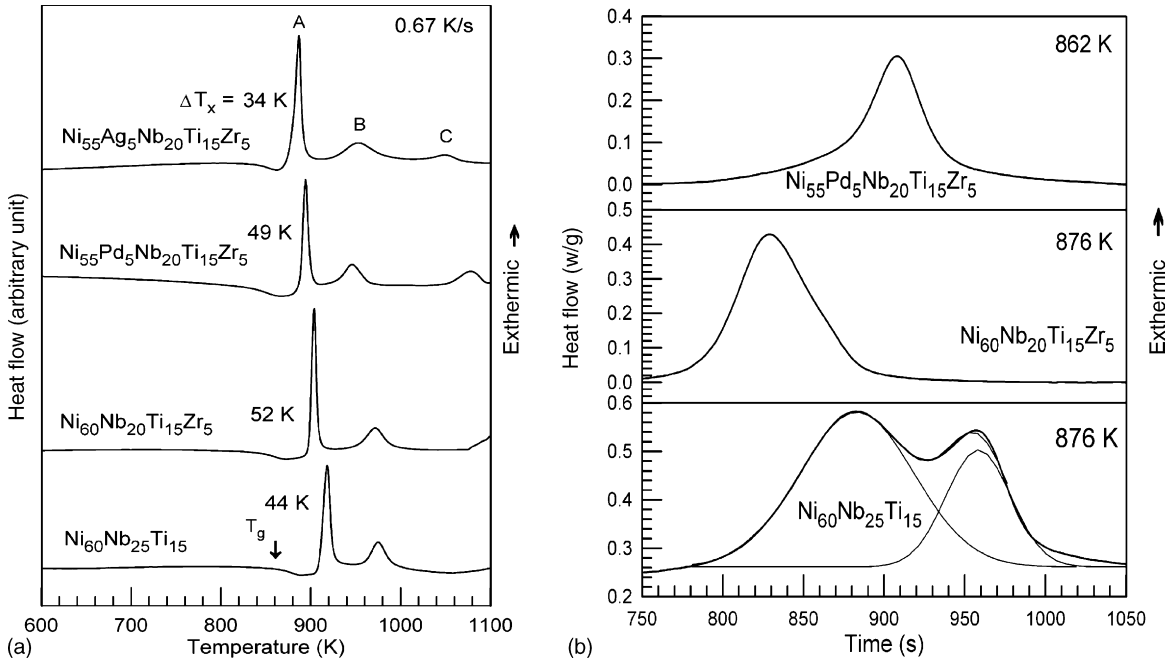

Fig. 2. (a) DSC and (b) isothermal calorimetry traces of the studied glassy alloys.

(crystallite size) calculated using (1 1 0) X-ray diffraction peak for $Ni_{60}Nb_{25}Ti_{15}$, $Ni_{60}Nb_{20}Ti_{15}Zr_5$, $Ni_{55}Ag_5Nb_{20}Ti_{15}Zr_5$ and $Ni_{55}Pd_5Nb_{20}Ti_{15}Zr_5$, are 60, 15, 13 and 9 nm, respectively.

These data correlate well with the TEM results presented for $Ni_{60}Nb_{25}Ti_{15}$ [17] and shown in Fig. 4 for the $Ni_{55}Pd_5Nb_{20}Ti_{15}Zr_5$ alloy annealed at 894 K for 480 s. The average particles size, as calculated from the bright-field TEM image in Fig. 4(a) for the $Ni_{55}Pd_5Nb_{20}Ti_{15}Zr_5$ alloy is 10 nm. The selected-area electron diffraction (SAED) pattern taken with a large selective diaphragm size (selected-area of about 1.3 μm in diameter) shows a halo from the residual glassy phase (Fig. 4(b) inset). This phase is also observed in the HRTEM image in Fig. 4(c). Nanobeam (probe size 5 nm) diffraction patterns shown in Fig. 4(d–g) indicate that some particles of cP2 TiNi phase transform to a martensitic so-called R-phase [20] (Fig. 4(f)) ($P3$ or $P\bar{3}1m$ space group) with lattice parameters $a = 0.73580$ nm and $c = 0.52855$ nm [21] (for a hexagonal cell). The formation of a definite fraction of the hR14 Ni_4Ti_3 phase with the lattice parameters $a = 1.124$ nm and $c = 0.5077$ nm [22] (in hexagonal coordinates) was also observed (Fig. 4(e and g)).

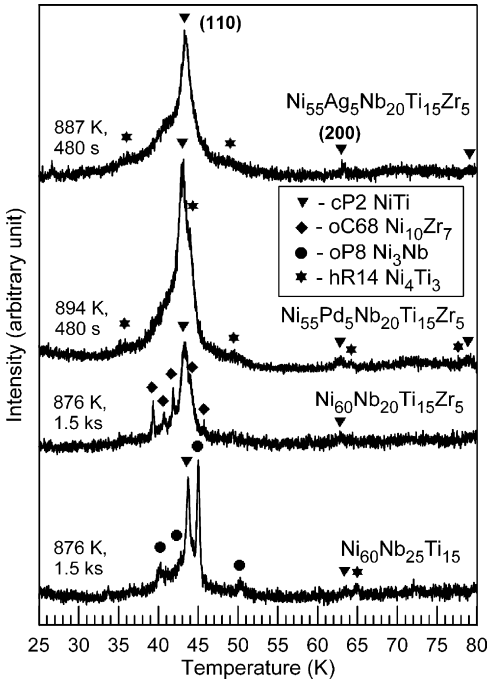

Fig. 3. X-ray diffraction patterns of the studied alloys after annealing. Annealing conditions (as indicated) correspond to the initial DSC exothermic peak.

X-ray EDS analysis showed that the nanoparticles in the $Ni_{55}Pd_5Nb_{20}Ti_{15}Zr_5$ alloy annealed at 894 K for 480 s have close composition from particle to particle. The cP2 TiNi particle was found to have the following composition: $Ni_{56}Pd_5Nb_{22}Ti_{12}Zr_5$. It is consistent with the fact that cP2 TiNi phase can dissolve Ni at high temperature.

No primary oP8 Ni_3Nb phase is observed in Zr and NM-bearing alloys while the formation of a definite fraction of the hR14 Ni_4Ti_3 phase leads to a non-symmetrical shape of the primary exothermic heat flow signals of these alloys (Fig. 2(b)). These results are also consistent with the XRD in Fig. 3 and the TEM data in Fig. 4.

oC68 $Ni_{10}(Zr, Ti, Nb)_7$ phase forms in all Zr-bearing alloys after the completion of all phase transformations on heating. The lattice parameters of this phase in the $Ni_{55}Pd_5Nb_{20}Ti_{15}Zr_5$ alloy after DSC up to 1150 K are $a = 0.907$ nm, $b = 0.891$ nm and $c = 1.186$ nm. Formation of $Ni_7(Zr, Ti, Nb)_2$ phase is also observed.

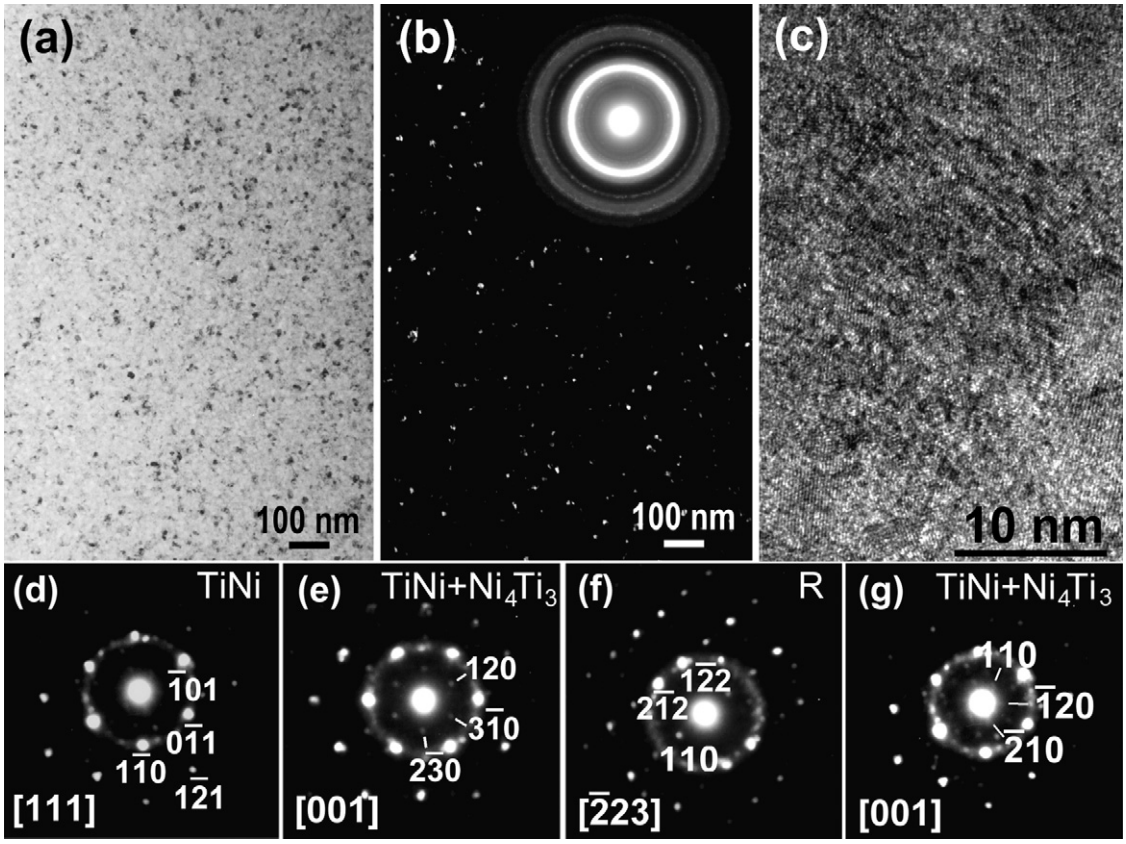

Fig. 4. (a) Bright-field, (b) dark-field images (*inset*: SAED) and (c) high-resolution TEM (HRTEM) image of $Ni_{55}Pd_5Nb_{20}Ti_{15}Zr_5$ glassy alloy annealed at 894 K for 480 s. Nanobeam diffraction patterns (probe size 5 nm) taken from (d) a cP2 TiNi particle, (e and g) a mixture of cP2 TiNi and hR14 Ni_4Ti_3 phases and (f) R-phase only in $Ni_{55}Pd_5Nb_{20}Ti_{15}Zr_5$ alloy annealed at 894 K for 480 s.

4. Discussion

As it is shown in Fig. 1 the glassy phase in $Ni_{55}Pd_5Nb_{20}Ti_{15}Zr_5$ alloy is free of nanoparticles contrary to some Cu-based alloys studied earlier which were found to be nanocomposites [see Refs. [23,24], for example].

Pd and Ag have different type phase diagrams with Ni. Ni and Pd exhibit unlimited mutual solid solubility with a singularity point while Ni–Ag phase diagram is monotectic immiscible system [25]. Nevertheless, as we found their influence on the devitrification behavior of Ni–Nb–Ti alloy is similar. The addition of NM together with Zr refines cP2 TiNi particles size by limiting their growth rate due to complication of chemical composition. This factor leads to an increase in the GFA.

According to Fig. 4 one can see that precipitation of a limited fraction of hR14 Ni_4Ti_3 phase, likely from cP2 TiNi, during the primary devitrification reaction in $Ni_{60}Nb_{20}Ti_{15}Zr_5$ and $Ni_{55}Pd_5Nb_{20}Ti_{15}Zr_5$ alloys and precipitation of the oC68 $Ni_{10}(Zr, Ti, Nb)_7$ phase in $Ni_{60}Nb_{20}Ti_{15}Zr_5$ alloy results in a non-symmetrical shape of the corresponding isothermal calorimetry traces (Fig. 2(b)).

It was reported previously [26] that the alloys exhibiting the supercooled liquid have a tendency to form primary metastable phases and phases with high crystallographic symmetry on devitrification. Formation of primary cP2 TiNi phase is in consistent with the earlier results.

Formation of the oC68 $Ni_{10}(Zr, Ti, Nb)_7$ phase in Zr-bearing alloys at a very small Zr content (5 at.%) can be explained based on the calculated mixing enthalpies for binary liquid systems which are −49, −35 and −30 kJ/mol for Ni–Zr, Ni–Ti and Ni–Nb systems, respectively [27,28], and high stability of this oC68 intermetallic compound [28].

5. Conclusions

The glassy single phase formed in Ni-based alloys is free of nanoparticles. The additions of Zr and NM to $Ni_{60}Nb_{25}Ti_{15}$ alloy prevent formation of oP8 Ni_3Nb phase upon crystallization and effectively refine cP2 TiNi particles size by limiting their growth rate owing to the formation of a complicated solid solution. This may be the reason for an increment in GFA of the NM containing alloys. cP2 TiNi → R transformation takes place in some particles. A definite fraction of hR14 Ni_4Ti_3 phase was also observed. The addition of Zr without NM initiates formation of oC68 $Ni_{10}Zr_7$ phase at the primary stage.

Acknowledgements

This work was supported by the Research and Development Project on Advanced Metallic Glasses, Inorganic Materials and Joining Technology and Priority Area on “Materials Science on Bulk Metallic Glasses” and the Grant-in-Aid (Wakate B) of

Ministry of Education, Sports, Culture, Science and Technology, Japan No.: 16760559.

References

[1] A. Inoue, Mater. Trans. JIM 36 (1995) 866.
[2] A. Inoue, Acta Mater. 48 (2000) 279.
[3] W.L. Johnson, MRS Bull. 24 (1999) 42.
[4] S. Yi, T.G. Park, D.H. Kim, J. Mater. Res. 15 (2000) 2425.
[5] J.K. Lee, S.H. Kim, S. Yi, W.T. Kim, D.H. Kim, Mater. Trans. JIM 42 (2001) 592.
[6] A. Inoue, W. Zhang, T. Zhang, Mater. Trans. 43 (2002) 1952.
[7] W. Zhang, A. Inoue, Mater. Trans. 43 (2002) 2342.
[8] T.C. Hufnagel, C. Fan, R.T. Ott, J. Li, S. Brennan, Intermetallics 10 (2002) 1163.
[9] W. Zhang, A. Inoue, Scripta Mater. 48 (2003) 641.
[10] H. Choi-Yim, D. Xu, W.L. Johnson, Appl. Phys. Lett. 82 (2003) 17.
[11] T. Zhang, A. Inoue, Mater. Trans. JIM 43 (2002) 708.
[12] M.H. Lee, J.Y. Lee, D.H. Bae, W.T. Kim, D.J. Sordelet, D.H. Kim, Intermetallics 12 (2004) 1133.
[13] D.V. Louzguine, A. Inoue, J. Non-Cryst. Solids 325 (2003) 187.
[14] D.V. Louzguine, A. Inoue, Scripta Mater. 48 (2003) 1325.
[15] D.V. Louzguine, A.R. Yavari, A. Inoue, Philos. Mag. 83 (2003) 2989.
[16] D.V. Louzguine, A. Inoue, J. Non-Cryst. Solids 337 (2004) 161.
[17] T. Shimada, D.V. Louzguine, J. Saida, A. Inoue, Mater. Trans. 46 (2005) 675–680.
[18] H. Hughes, J. Iron Steel Inst. Lond. 2003 (1965) 1019.
[19] S.S. Gorelik, U.A. Skakov, L.N. Rastorguev, X-ray and Electron-optic Analysis, MISIS, Moscow, 1994, p. 328 (in Russian).
[20] S. Miyazaki, S. Kimura, K. Otsuka, Philos. Mag. A 57 (1988) 467.
[21] T. Hara, T. Ohba, E. Okunishi, K. Otsuka, Mater. Trans. JIM 38 (1997) 11.
[22] T. Saburi, S. Nenno, T. Fukuda, J. Less-Common Met. 125 (1986) 157–161.
[23] Y. Chen, T. Zhang, W. Zhang, D. Ping, K. Hono, A. Inone, T. Sakurai, Mater. Trans. 43 (2002) 2647.
[24] J.Z. Jiang, B. Yang, K. Saksl, H. Franz, N. Pryds, J. Mater. Res. 18 (2003) 895.
[25] W.F. Gale, T.C. Totemeier (Eds.), Smithells Metals Reference Book, eighth ed., Elsevier Butterworth-Heinemann Ltd., Oxford, UK, 2004, pp. 11–20.
[26] D.V. Louzguine, A. Inoue, Mater. Sci. Eng. A 375–377 (2004) 346–350.
[27] F.R. De Boer, R. Boom, W.C.M. Mattens, A.R. Miedema, A.K. Niessen, Cohesion in Metals, North-Holland, Elsevier Science Publishers, 1988, pp. 31–33.
[28] A. Takeuchi, A. Inoue, Mater. Trans. JIM 41 (2000) 1372.